Cerebral Cortex April 2015;25:1004–1019
doi:10.1093/cercor/bht291
Advance Access publication October 31, 2013

Ventral Fronto-Temporal Pathway Supporting Cognitive Control of Episodic Memory Retrieval

Jennifer Barredo[2], Ilke Öztekin[4] and David Badre[1,2,3]

[1]Department of Cognitive, Linguistic, and Psychological Sciences, [2]Neuroscience Graduate Program, [3]Brown Institute for Brain Sciences, Brown University, Providence, RI 02912, USA and [4]Department of Psychology, Koç University, Sariyer 34450, Istanbul, Turkey

Address correspondence to Jennifer Barredo, Box G-LN, Brown University, Providence, RI 02912-1978, USA. Email: Jennifer_Barredo@brown.edu

Achieving our goals often requires guiding access to relevant information from memory. Such goal-directed retrieval requires interactions between systems supporting cognitive control, including ventrolateral prefrontal cortex (VLPFC), and those supporting declarative memory, such as the medial temporal lobes (MTL). However, the pathways by which VLPFC interacts with MTL during retrieval are underspecified. Prior neuroanatomical evidence suggests that a polysynaptic ventral fronto-temporal pathway may support VLPFC–MTL interactions. To test this hypothesis, human participants were scanned using fMRI during performance of a source-monitoring task. The strength of source information was varied via repetition during encoding. Single encoding events should produce a weaker memory trace, thus recovering source information about these items should demand greater cognitive control. Results demonstrated that cortical targets along the ventral path—anterior VLPFC, temporal pole, anterior parahippocampus, and hippocampus—exhibited increases in univariate BOLD response correlated with increases in controlled retrieval demand, independent of factors related to response selection. Further, a functional connectivity analysis indicated that these regions functionally couple and are distinguishable from a dorsal pathway related to response selection demands. These data support a ventral retrieval pathway linking PFC and MTL.

Keywords: functional connectivity, retrieval, VLPFC

Introduction

Efficient retrieval of long-term memories relevant to one's current behavioral goals depends on cognitive control mechanisms supported by prefrontal cortex (PFC; Jetter et al. 1986; Stuss and Benson 1986; Janowsky et al. 1989; Moscovitch 1994; Shimamura 1995). There are at least 2 ways that cognitive control processes can interact with memory retrieval (Badre and Wagner 2007; Benjamin 2007). First, cognitive control mechanisms can operate on the "output" of the memory system, such as monitoring retrieved details with respect to one's current context and decision criteria, and engaging in response selection processes based on retrieved content. Second, cognitive control mechanisms can influence access to memory itself, increasing the likelihood that task-relevant information is successfully retrieved. In the context of episodic retrieval, this latter "controlled retrieval" process may operate by elaborating cues or activating stored semantic representations, thereby shaping the input to MTL systems and increasing the likelihood of recovering relevant memories.

Neuroimaging experiments manipulating controlled retrieval consistently observe activation in anterior ventrolateral PFC (aVLPFC, Brodmann area [BA] 47; Wagner et al. 2001; Badre et al. 2005; Badre and Wagner 2007). During semantic retrieval, aVLPFC activation is often accompanied by activation in lateral temporal regions supporting storage of lexical/semantic representations (Badre et al. 2005; Dobbins and Wagner 2005; Wimber et al. 2008; Han et al. 2012); while in the episodic domain, co-activation of VLPFC and hippocampal cortex (HPC) in the medial temporal lobes (MTL) has been observed (Dobbins et al. 2003; Maril et al. 2003; Simons and Spiers 2003).

The co-activation of aVLPFC and its putative temporal lobe targets is potentially consistent with a controlled retrieval process that influences the activation of information from long-term stores (Badre and Wagner 2007). Currently, however, the neural pathways that support any cortico-cortical interactions between aVLPFC and MTL are unknown. As aVLPFC is not connected to MTL monosynaptically, control signals are likely propagated along polysynaptic pathways with multiple intermediate targets. The goal of the present work is to identify a pathway supporting these cortico-cortical interactions during controlled episodic retrieval.

One such polysynaptic pathway might be comprised of ventral PFC projections to the anterior temporal cortex (aTC), including those along the uncinate fasciculus, and projections from lateral temporal cortex to MTL. Projections from ventral PFC/orbitofrontal cortex to aTC and anterior parahippocampal gyrus (aPHG) have been identified using tracers in nonhuman primates (Petrides and Pandya 2001) and in human dissections (Kier et al. 2004), while tracer work in rodents and monkeys has established that aTC and aPHG are densely interconnected as are aPHG and the HPC and neighboring entorhinal cortex (Suzuki and Amaral 1994; Furtak et al. 2007; Burwell and Agster 2008). Additionally, functional connectivity analysis of low-frequency blood oxygen level–dependent (BOLD) fluctuations collected during rest has provided evidence of task-independent correlation among approximately these ventral path regions within broader functional networks (Vincent et al. 2008; Yeo et al. 2011). Thus, although aVLPFC, aTC, aPHG, and HPC have not been collectively implicated in the cognitive control of retrieval, we hypothesize that these regions form a ventral pathway permitting aVLPFC to influence MTL during controlled retrieval.

Importantly, however, functionally defining pathways involved in controlled retrieval is complicated by the observation that there are multiple PFC mechanisms that can influence retrieval performance without necessarily affecting retrieval itself. FMRI evidence has associated PFC, including regions of VLPFC and dorsolateral PFC (DLPFC), with postretrieval processes related to decision-making, response selection, and monitoring (Thompson-Schill et al. 1997; Fletcher and Henson 2001; Dobbins et al. 2002, 2003; Dobbins and Han 2006;

Hayama and Rugg 2009; Öztekin and Badre 2011). For example, previous fMRI studies have demonstrated that activation in mid-VLPFC (pars triangularis [~BA45]) is correlated with the demand for a general selection process across multiple types of semantic memory judgments (Badre et al. 2005). And, the effects of postretrieval operations in mid-VLPFC can be dissociated from those related to controlled retrieval in aVLPFC (Badre et al. 2005; Gold et al. 2006). Thus, manipulations used to identify a pathway specific to controlled retrieval must isolate demands related to memory access from those correlated with output-stage control demands.

Furthermore, postretrieval operations might leverage pathways outside of VLPFC. Prior work has implicated regions of inferior parietal cortex, DLPFC, and frontopolar cortex in postretrieval monitoring, decision-making, and response selection during memory tasks (Dobbins and Wagner 2005; Badre and Wagner 2006; Hayama and Rugg 2009; Vilberg and Rugg 2012). Indeed, these regions might, themselves, interact as a distinct network. In fact, DLPFC and subregions of parietal cortex are often correlated at rest as a network sometimes termed the fronto-parietal control system (Dosenbach et al. 2007; Vincent et al. 2008; Yeo et al. 2011). Moreover, a recent parcellation of functional networks based on resting-state fMRI correlations from a large sample included mid-VLPFC in the ventral boundary of this fronto-parietal network (Yeo et al. 2011). Hence, characterizing a network supporting controlled retrieval should also explore its relationship to these broader cognitive control networks.

Here, we test the hypothesis that aVLPFC, MTL, and intermediate structures along the ventral path comprise the primary network supporting PFC–MTL interactions during controlled episodic retrieval. To test this, we manipulated memory strength within an exclusion source memory task (Jacoby 1991; McElree et al. 1999, Fig. 1) that controls for contributions of postretrieval response selection processes. We predicted that regions along the ventral pathway would demonstrate selective BOLD increases as a function of controlled retrieval demands and would show greater functional connectivity with one another relative to regions outside of this pathway.

Materials and Methods

Participants

Nineteen participants (11 females, mean age 24 years) were included in the study. All participants were right-handed, native English speakers with no history of neurological or psychiatric diagnoses, use of medications with potential vascular or central nervous system effects, or contraindication for MRI. Three additional participants were enrolled, but their data were excluded because of either excessive head movement (>3 mm; 2 participants) or scanner failure (1 participant). One additional subject had to be excluded from the functional connectivity analysis because of a counterbalancing error that led to uneven block lengths precluding good assessment of a stable connectivity signal over some of the blocks. Thus, 18 subjects were used in the functional connectivity analysis. Participants were remunerated $15/h. Informed consent was obtained in accord with procedures approved by the Institutional Review Board of the Research Protections Office at Brown University.

Logic and Design

To test the involvement of the ventral pathway in controlled retrieval, we scanned participants during a Source exclusion task, in which they decided whether or not they had performed 1 of 2 semantic decisions (Size or Organic) with individual words encountered during an earlier encoding phase (Fig. 1*A*; see "Behavioral Protocol" for full details about the encoding phase). The design of the Source exclusion task included the crossing of 2 factors, termed Congruency and Strength, which allowed us to distinguish brain regions responding to demands on controlled retrieval versus those related to response selection processes. For clarity, we describe the logic of the design in this section. Details regarding stimuli and specifics of the behavioral protocol (trial numbers, durations, etc.) are provided in Figure 1 and in the "Stimuli" and "Behavioral Protocol" sections of the Materials and Methods that follow this one.

At the beginning of a block of source retrieval trials, subjects were cued with one target source task, either Size or Organic. They were instructed to indicate, using a Yes/No keypress, whether each subsequently presented word in that block was performed with the target source task or not. Importantly, Old words were presented that had been previously encountered with the target source task, and other Old words were presented that had been encountered with the nontarget source task. Old words for which the encoding decision matched the target source task were positively endorsed with a "Yes" response, whereas Old words encoded with the nonmatching source task were

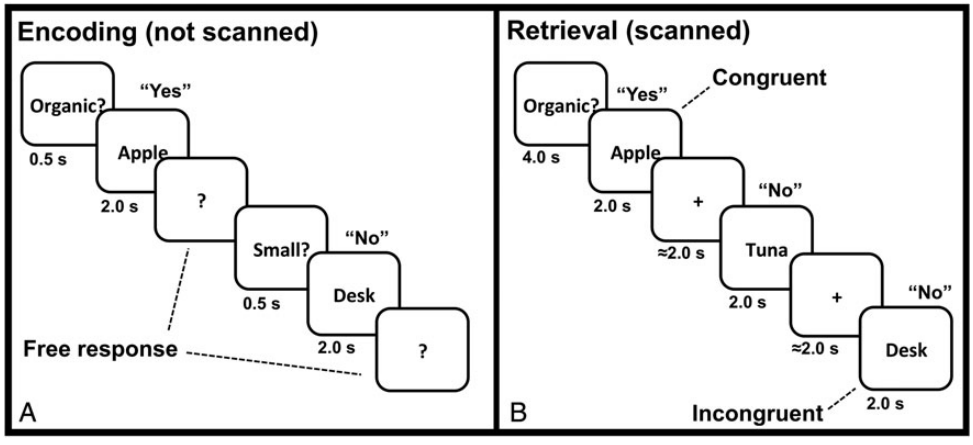

Figure 1. Schematic of the trial events during the encoding and Source tasks. (*A*) During encoding, trials were initiated by pressing a keyboard space bar that prompted the display of a semantic decision cue (0.5 s). This was followed by the display of a word (2 s), followed by a prompt (?) that remained on the screen until a response was made. Participants had unlimited time to answer "Yes" or "No" for that item with respect to the orienting question and the next trial cycle did not begin until it was initiated by the participant. (*B*) During source retrieval blocks, participants reported whether presented words were encountered at encoding with the orienting question displayed at block start. Target source task prompts (either "Organic?" or "Small?") were displayed for 4 s at the start of each block, and were followed by a 12 s baseline and then word targets were presented for 2 s each. Participants responded "Yes" or "No" during the 2 s target presentation. A jittered ITI separated retrieval trials within blocks.

correctly rejected with a "No" response. Previously unseen "New" items were also rejected with a "No" response.

These response rules can be conceptualized as a "Congruency" manipulation that places demands on response selection processes. Specifically, consider that any evidence of an item having been encountered previously (i.e., evidence of oldness), whether through familiarity or recollection, can drive a tendency to endorse the item and respond "Yes" (see Supplementary Material for a detailed discussion of the causes of this tendency). This response tendency should scale with the strength of the evidence of oldness. Thus, Old words that were not encountered with the target source task elicit a response compatibility effect, in that the participant must respond "No" in the presence of a tendency to respond "Yes" because the item is old. This response competition places greater demands on response selection processes for these "Incongruent" items. In contrast, Old items that were performed with the target source task do not feature response competition, and so these "Congruent" items place lower demands on response selection.

Second, a Strength manipulation at encoding varied the accessibility of individual memory representations, thereby affecting the demand for controlled retrieval. Specifically, some words were encountered 5 times with their respective source task during encoding (Strong), whereas others were encountered only once (Weak). This Strength manipulation is hypothesized to have 2 effects during retrieval: 1) Higher Strength results in greater retrieval fluency, and so easier recollection. Thus, it should be easier to retrieve details that are diagnostic of which semantic decision was performed with a Strong item. Accordingly, regions involved in controlled retrieval will be more engaged for Weak than Strong items in an effort to recover these diagnostic details when source evidence is scarce. 2) Strength also interacts with the response selection process as described above. Specifically, in contrast to the ease of memory access, the rejection of Strong Incongruent items should be harder than Weak Incongruent items at the response level because greater evidence of oldness drives a stronger tendency to respond "Yes." Conversely, it will be easier to endorse Strong Congruent items than Weak Congruent items.

From this logic, the crossing of Strength with Congruency allowed us to distinguish brain regions that respond to controlled retrieval independently from those related to response selection demands. First, regions related to controlled retrieval should show a main effect of Strength and no interaction with Congruency. Consider that for each Old item, participants must recollect details from the encoding event that are diagnostic of which encoding task was performed with that item. As participants do not know in advance whether an Old item is Congruent or Incongruent, controlled retrieval processes would be engaged for both trial types in order to guide recollection of diagnostic source details. The ease with which such details are recovered should vary with Strength. In other words, participants may recollect details confirming that a Congruent item was encountered with the target source task, or they may retrieve a detail that confirms that an Incongruent item was encountered in the nontarget source task. In either case, retrieving this diagnostic detail will be more difficult and so will require more controlled retrieval for Weak than Strong items. Thus, regions supporting controlled retrieval should show a main effect of Strength but no crossover interaction with Congruency (It is possible that Strong items would tend to elicit controlled retrieval attempts more frequently than Weak items, because they are likely to be judged as familiar more often. However, this would occur equivalently for Congruent and Incongruent items and would be inversely related to the ease with which this process retrieves a diagnostic detail. Thus, to the degree that the average demand of frequent but easy controlled retrieval events [Strong trials] is less than the infrequent but harder retrieval events [Weak trials], Weak trials will elicit greater activation in controlled retrieval regions than Strong items on both Congruent and Incongruent trials.).

In contrast, regions involved in response selection will show an interaction of Strength with Congruency. As described above, despite the relative ease with which a diagnostic source detail can been recovered in the case of Strong items, the selection of a "No" response for Strong Incongruent items will be more difficult than for Weak items as a result of response competition. In contrast, it will not only be easier to retrieve diagnostic details for Strong Congruent items, but it is also easier to choose the "Yes" response. Thus, a region of the brain that is sensitive to response selection demands in this experiment will show an interaction between Strength and Congruency. (It should be noted that given the crossover nature of this interaction, a main effect of Congruency is not necessarily predicted by such a model.)

Following from this logic, we predicted that: 1) the aVLPFC would show greater activation for Weak than Strong items independent of Congruency. 2) Additional regions along the a priori-defined ventral path such as aTC, aPHG, and HPC would also show Weak > Strong effects independent of Congruency. 3) Voxels showing this univariate effect would form a coherent network as assessed through functional connectivity analysis. 4) Regions outside of the ventral pathway that are involved in postretrieval response selection processes—such as mid-VLPFC, DLPFC, and intraparietal sulcus—would show an interaction between Strength and Congruency.

Stimuli

Word stimuli used for the memory task were English nouns taken from a set that was previously normed for their organic (organic/inorganic) and size (large/small) properties (Race et al. 2009), as well as word frequency and mean length (Kucera and Francis 1967). Four hundred words were evenly divided into 4 list categories (small/organic, large/organic, small/inorganic, and large/inorganic). Each experimental condition was assigned a word list including an even number of words from each category. Assignment of lists to conditions was counterbalanced across participants.

Behavioral Protocol

The encoding phase of the experiment was performed outside of the MRI scanner on a Macintosh laptop. During encoding (Fig. 1*A*), participants were asked to make semantic decisions about 240 words. Each trial began with the presentation of a cue (Organic?/Size?) for 500 ms. The cue indicated whether the item named by a subsequently presented noun should be categorized as larger/smaller than a shoebox (Size decision) or was organic/inorganic (Organic decision). Target words were displayed for 2000 ms. Half of the item words were presented 5 times during the encoding task, strengthening memory for these item-judgment pairs (Strong). The remaining items were encountered only once (Weak). Strong items were always repeated with the same semantic decision. Participants could respond at any time following word offset via laptop key press. In this way, viewing time was equated across all words. Following a response, there was a participant-determined intertrial interval (ITI) before presentation of the next decision cue. The ITI ended when participants pressed the spacebar prompting the start of the next trial. Participants were instructed to respond as quickly but as accurately as possible for each item. The encoding task was comprised of 720 trials divided into 2 blocks. During encoding, participants were given no indication that their memory would subsequently be tested for the words encountered in this phase.

During the scanned retrieval phase (Fig. 1*B*), participants performed 20 blocks of the Source task (10 trials/block) divided among 4 runs (5 blocks/run). At the start of Source blocks, participants were presented with a cue naming one of the semantic decisions (either Size? or Organic?). This cued them to report whether they had made that semantic decision during encoding with each item in the upcoming block. Instruction cues were displayed at the beginning of each block for 4 s, followed by a 12 s fixation baseline before presentation of the retrieval targets. Each retrieval target was displayed for 2 s followed by a variable (ITI length = 0, 2, 4, 6, or 8 s; mean = 3.8 s, mode = 2 s). ITI was randomized between conditions, and there were no differences in the mean ITI between conditions ($F = 1.06$, $P = 0.4$).

Participants were instructed to respond within the 2-s display window and were told that responses made after word offset were treated as nonresponses. Participant responses were made using an MRI-safe button box during scanning; responses made after display offset were counted as nonresponse trials. The order of trials and duration of jittered ITIs within a block was determined by optimizing the efficiency of the design matrix so as to permit estimation of the event-related response (Dale 1999).

One hundred sixty words previously encountered during encoding were seen in Source recognition blocks (the remaining 80 of the words from encoding were encountered during blocks of Item recognition). Forty words not encountered at encoding (New words) were also pseudo randomly mixed into Source blocks at a rate of 2 New words per block. Old words were equally likely to be Strong or Weak.

An Item recognition task was also included during the scan during which participants decided whether individually presented words had been seen during the earlier encoding phase. Within a scanning run, participants alternated between Item and Source blocks with order counterbalanced across the experiment. However, as the Item task contributed little to the objectives of the present study, we focus on the Source task in the present report. See Supplementary Material for details regarding the Item task, including methods, behavioral, and neuroimaging results.

In order to permit functional connectivity analysis, Strength was blocked. Thus, the 5 blocks of the Source task within each run were divided between Strong and Weak. As this is an odd number and required one more block of either Strong or Weak for each run, the frequency of these blocks was balanced at the session level and the order was counterbalanced across participants.

Across blocks of the Source memory task, old items could have been previously encountered during the target source task (Congruent Items) or with the nontarget source task (Incongruent Items) with equal likelihood. Congruent and Incongruent items were balanced across blocks, runs, and memory Strength within the source condition. Thus, the fMRI experimental design consisted of 5 experimental conditions: strong Source Congruent, Weak Source Congruent, Strong Source Incongruent, Weak Source Incongruent, and New. There were 40 trials per condition across the experiment. For a summary of design details, see Supplementary Table S2.

MRI Procedures

Whole-brain images were collected using a Siemens 3T TIM Trio MRI system equipped with a 32-channel head coil. High-resolution T_1-weighted anatomical images were collected for registration and visualization (multiecho magnetization prepared rapid acquisition gradient echo). Functional MRI data were collected from participants during performance of the retrieval task, and were acquired in 4 runs of 371 volume acquisitions, using a gradient-echo echo-planar sequence ($3 \times 3 \times 3$ mm, TR = 2.0 s, TE = 30 ms, flip angle = 90°, 33 axial slices, 10% interslice gap, 4 dummy scans). Functional MRI data for resting-state analysis were collected from participants prior to the retrieval task, and were acquired in 1 run of 124 volume acquisitions optimized for functional connectivity analysis, using a gradient-echo echo-planar sequence ($3 \times 3 \times 3$ mm, TR = 3.0 s, TE = 30 ms, flip angle = 85°, 47 transverse slices, no skip, no dummy slices, fat saturation on). Head movement during scanning was limited by the use of foam padding in the scanner headrest. Participants viewed the experimental display through a back projection system and mirror attached to the MRI head coil. During the resting-state scans, participants were asked to remain still and keep their eyes open while viewing a blank black screen. All experimental scripts were programmed using the Psychophysics Toolbox (http://psychtoolbox.org/) for MATLAB® (The MathWorks, Natick, MA, USA) and were run on Macintosh computers.

Univariate fMRI Analysis

Functional imaging data from the memory task were processed using SPM5 (Wellcome Department of Cognitive Neurology, London). Quality assurance included checks for outliers or artifacts in both volume and slice-to-slice variance in the global signal. Data were evaluated as high quality, thus no corrections were applied. Preprocessing of functional images for univariate analysis included the following steps: 1) Slice-timing correction by resampling subsequent slices in time to match the first slice; 2) motion correction using second-degree B-spline interpolation; 3) normalization of functional and anatomical images to Montreal Neurological Institute (MNI) stereotaxic space using a 12-parameter affine transformation along with a nonlinear transformation using a cosine basis set (final voxel resolution $3 \times 3 \times 3$); 4) and spatial smoothing with an 8-mm full-width at half-maximum isotropic Gaussian kernel.

A statistical model of the task data was constructed under the assumptions of the general linear model. For correct trials, regressors were constructed based on the memory Strength (Strong/Weak), and Congruency (Incongruent/Congruent), along with a separate regressor for New Items. Failures to endorse target source items (Misses), endorsement of nontarget source items (False Alarm [FA]), or endorsement of New items (FA) were classified as errors. These error types were coded separately for the behavioral analysis. However, as few errors were made in some conditions, there were insufficient trials to model different error types separately in fMRI. Thus, incorrect trials were grouped together into an error regressor. This allowed us to remove variance due to errors as a nuisance variable, but not to distinguish signal related to the different error types. Additional nuisance regressors for the onset of an instruction cue, an unanalyzed motor task, and the Item recognition task were also included in the model (see Supplementary Material for details on the unanalyzed motor task and the Item recognition task).

A second GLM was also estimated that was identical to the one described above except that we coded New items as Strong or Weak depending on whether they were encountered within a block of Strong or Weak items. This GLM was used to conduct control analyses that tested for set-level effects such as a shift in response criterions between blocks, potentially introduced by the blocking of memory strength. As familiarity is equivalent across New items regardless of whether they were encountered in the context of a Strong or Weak block, there should be no difference in the BOLD signal elicited by their contrast. All regressors were generated by convolving 2-s epochs at each event onset with a canonical hemodynamic response function and its temporal derivative. Run-to-run variance and low-frequency signal components (<0.01 Hz) were treated as confounds. Within-subject effects were estimated using linear contrasts. For whole-brain analyses, these contrast beta estimates were entered into a second-level random effects analysis, using a 1-sample *t*-test against a contrast value of 0 at each voxel.

ROIs used in subsequent analyses (both univariate ROI and seed-based functional connectivity) were defined in an unbiased fashion using 4 methods (see Table 1). 1) To test regions of aVLPFC and mid-VLPFC previously related to controlled retrieval and postretrieval selection, ROIs were defined based on the exact voxel definition from a prior study of these functions from our laboratory (Badre et al. 2005). 2) To test regions previously identified in the "fronto-parietal control system" and "the default network," we defined a set of ROIs as 8-mm spheres around peak coordinates in these networks reported in a prior

Table 1
Description of seeds used for ROI and functional connectivity analysis

Seed	Definition Criteria	MNI/AAL coordinates	Brodmann's area (BA)
Strength modulated ventral path seeds			
aVLPFC	Semantic retrieval. Badre et al. (2005).	−51, 27, −3	47
aTC	Temporal pole AAL mask, modified after Blaizot et al. (2010).	−39, 14, −22	38
aPHG	Parahippocampal AAL mask, modified after Kahn et al. (2008).	−22, −9, −28	35
HPC	Hippocampal AAL mask	−32, −24, −12	
Proximate ventral path seeds, nonstrength modulated			
Mid-VLPFC	Semantic retrieval. Badre et al. (2005).	−51, 15, 33	45
Exploratory seeds—fronto-parietal control network			
PFCl	Intrinsic connectivity. Yeo et al. (2011)	−38, 33, 16	46[a]
PFClp	Intrinsic connectivity. Yeo et al. (2011)	−45, 29, 32	9/46v[a]
IPS	Anatomical (also termed IPS3l), after Scheperjans, Eickhoff et al. (2008); Scheperjans, Hermann et al. (2008)	−35, −56, 42	~39/7
Exploratory seeds—default network			
PFCdm	Intrinsic connectivity. Yeo et al. (2011)	−4, 49, 32	9, Medial
PFCdp	Intrinsic connectivity. Yeo et al. (2011)	−44, 15, 48	9, Lateral
PGpd	Anatomical, after Caspers et al. (2006); Caspers et al. (2008)	−49, −63, 45	39

[a]As defined in Petrides et al. (2012).

functional connectivity study (Yeo et al. 2011). 3) To define ROIs in aTC, aPHG, and HPC, we started with broad anatomical definitions based on the Automatic Anatomical Labeling masks (AAL—Tzourio-Mazoyer et al. 2002) and refined these using landmarks reported in the anatomical literature (aTC: Blaizot et al. 2010; aPHG: Kahn et al. 2008).

Task-Based Functional Connectivity Preprocessing and Analysis

Functional connectivity preprocessing was performed on slice-time corrected data (SPM5). Images were sorted by Strength (Strong Source, Weak Source) and concatenated within a functional run into a 4D image for further analysis. Subsequent preprocessing and analysis steps were conducted with the 1000 Functional Connectomes (http://fcon_1000.projects.nitrc.org/) data processing pipeline for functional connectivity analysis. These scripts use functions from both the AFNI (http://afni.nimh.nih.gov/afni) and FSL (http://www.fmrib.ox.ac.uk/fsl/) fMRI image processing packages. Images were motion-corrected, skull-stripped, registered to MNI space, resampled to 2 mm voxels, smoothed (8-mm Gaussian kernel), and band-pass filtered (high pass = 0.03 Hz, low pass = 0.1 Hz). Subjects' own anatomical images were used to define CSF and white matter in native space to permit calculation of nuisance regressors for global signal, white matter, and CSF along with regressors for the 6 motion parameters. After within-run regression, residuals were extracted and mean-corrected. Finally, linear and quadratic trends were removed during run-by-run ordinary least-squares regression. The resulting residuals were resampled to MNI space.

Seed-based functional connectivity assessed the correlation in signal between seed and target brain regions. Our seeds included the ROIs from our univariate analysis described above, and an additional set of ROIs that we used to explore how our ventral path ROIs might couple with either known functional networks defined from resting-state correlations (see Table 1). During first-level analysis, the signal time series over the session for each ROI was extracted, and Pearson's product moment correlations computed the pairwise regional correlation between the time course from each ROI and all other voxels in the volume. The resulting correlation map was *Z*-transformed (Fisher's transformation). Individual subject's statistical maps were entered into a second-level random effects analysis in SPM, using a 1-sample *t*-test against a contrast value of 0 at each voxel. Voxelwise group effects were considered at a $P < 0.05$ FDR-corrected threshold. To remove singleton or very small clusters, height-corrected maps were extent thresholded at 5 contiguous voxels.

Conjunction maps were used to identify voxels where connectivity across multiple seed regions surpassed FDR-correction. Maps were generated by extracting clusters of 5 or more contiguous voxels that were significant at $P < 0.05$ after FDR-correction from a given functional connectivity seed map. A binarized map was created by assigning all above-threshold voxels a 1 and all others a value of 0. These binary seed maps were then combined using an "AND" conjunction during the analysis, thus only voxels above FDR-threshold in all seeds used in a given conjunction were regarded as reliable. This approach provides a test of "valid conjunction" among the connectivity maps (Nichols et al. 2005).

Resting-State Functional Connectivity Preprocessing and Analysis

The analysis of functional connectivity during an ongoing task comes with the caveat that the task itself could act as a third variable driving apparent coordination between 2 regions. Even removing task-related activity or filtering high-frequency signal components leaves open the possibility that some aliased signal or residual task activity remains to drive correlations. Thus, we conducted a complementary functional connectivity analysis on independent fMRI data collected during the resting state.

Analysis of the resting-state data was identical to methods used in the functional connectivity analysis of task data with 2 exceptions (see Task-based functional connectivity preprocessing and analysis). First, resting-state data were collected in one sequential acquisition so the concatenation step was not performed. We did, however, drop the first 4 acquisitions to allow the fMRI signal to stabilize since dummy scans are not collected as part of the resting-state acquisition protocol. Second, least square regression was conducted over one run only, as data were collected in one run.

Results

Behavioral Performance

Response time (RT) and error rates provided initial evidence that the Strength and Congruency manipulations modulated control demands as predicted (Table 2 and Fig. 2). As expected, when memory Strength was Weak, retrieval was less accurate, presumably because source evidence was less available. Accuracy (Hits + CR) was lower for Weak compared with Strong items ($F_{1,18} = 14.0$, $P < 0.001$; Fig. 2*A*). Other main effects on Accuracy and RT were not reliable ($P > 0.09$). Importantly, as predicted, memory strength interacted with Congruency in both RT ($F_{1,18} = 10.6$, $P < 0.005$; Fig. 2*B*) and Accuracy ($F_{1,18} = 71.5$, $P < 0.001$; Fig. 2*A*). Specifically, within the Congruent condition, Strong cues were endorsed more accurately ($t_{(18)} = 12.2$, $P < 0.001$) and faster ($t_{(18)} = 12.4$, $P < 0.001$) than Weak cues. In contrast, in the Incongruent condition, Weak cues were responded to more accurately ($t_{(18)} = 2.6$, $P < 0.01$) and faster than Strong cues ($t_{(18)} = 2.7$, $P < 0.05$). This crossover interaction between Strength and Congruency is consistent with a prepotent tendency to endorse highly familiar targets. Strong Incongruent false alarms items were responded to more quickly (1078 ms) than Strong Incongruent correct rejections (1138 ms; $t_{(18)} = 2.1$, $P = 0.05$), further consistent with a response tendency that derives from rapid automatic retrieval.

We next sought to rule out effects of blocking memory Strength. Strength was blocked in order to permit functional connectivity analysis. However, it is possible that the blocking of Strength could have elicited differences in response bias between Strong and Weak blocks. As a test of criterion shifting between blocks, we probed differences in FA rates to New items between Strength conditions (Stretch and Wixted 1998; Verde and Rotello 2007). New items were mixed with Old items in both Strong and Weak blocks. But, as New items were not encountered at encoding, it is reasonable to assume that the evidence distributions of these items are equivalent across Strength conditions. Thus, any change in FA rates to New Items between Strong and Weak blocks would be due to a criterion shift. However, we did not find evidence of such a difference ($t_{(18)} = 0.04$, $P = 0.97$).

Table 2
Source recognition memory performance

Proportion responses (SE)	Strong	Weak
Congruent Old		
Hits	0.81 (0.02)	0.54 (0.03)
Misses	0.19 (0.02)	0.46 (0.03)
Incongruent Old		
Correct rejections	0.56 (0.04)	0.66 (0.03)
False alarms	0.44 (0.04)	0.34 (0.03)
New		
Correct rejections	0.86 (0.03)	0.86 (0.03)
False alarms	0.14 (0.03)	0.14 (0.03)
Reaction times in ms (SE)		
Congruent	1058 (23)	1144 (27)
Incongruent	1138 (28)	1102 (34)
New	1083 (22)	1009 (21)

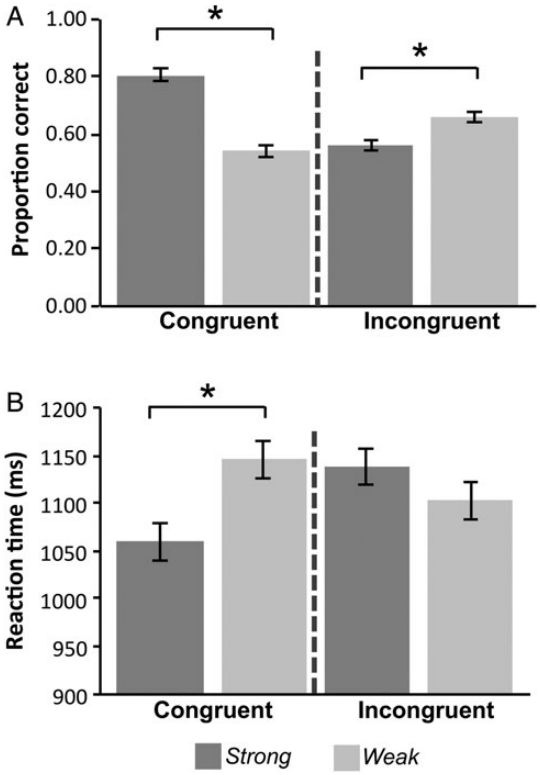

Figure 2. Behavioral results (Accuracy and RT) for Congruency and Strength conditions of the Source task. Congruency and Strength produced a crossover interaction in Accuracy and RT, such that Weak Congruent trials were associated with lower accuracy and slower RT than Strong Congruent, but Strong Incongruent produced worse performance than Weak Incongruent. Error bars depict within-subject standard error (*$P < 0.05$).

Effects of Memory Strength Along the Ventral Path

In general, patterns of activation across conditions in the a priori target regions along the ventral pathway (aVLPFC, aTC, aPHG, and HPC) were consistent with the controlled retrieval hypothesis; namely a main effect of memory Strength that did not interact with Congruency (Fig. 3). Integrated percent signal change (IPSC) increased under conditions of Weak relative to Strong memory strength in ROIs located within aVLPFC, aTC, and aPHG (F's > 5.1, $P < 0.05$; Fig. 3*A–C*). HPC showed the same pattern of Weak greater than Strong across Congruency conditions, though in this ROI, the effect was marginal ($F_{1,18} = 3.1$, $P = 0.09$; Fig. 3*D*). In all ROIs along the ventral path, there were neither main effects of Congruency (F's$_{1,18} < 1.1$) nor evidence of an interaction of Congruency with memory Strength (F's$_{1,18} < 0.5$). In order to establish that the ventral path regions are engaged in controlled memory retrieval success, we next contrasted Weak trials across Congruency conditions against New trials (Fig. 3). Again, Weak items presumably place the greatest demands on controlled retrieval to verify the source. In contrast, New items are also low evidence events, but are not associated with successful retrieval. Weak items elicited greater activation than New items in aVLPFC, aTC, and aPHG (t's > 2.6, P's < 0.05). HPC again showed a marginal effect ($t_{(18)} = 1.7$, $P = 0.1$).

Finally, to again rule out concerns that the blocking of Strength conditions might have induced participants to approach Strong and Weak blocks using different set-level retrieval strategies or criteria, we constructed an additional GLM that coded New items as Strong or Weak based on the block in which they were encountered. Comparison of New items encountered during Strong versus Weak blocks at a lenient threshold ($P < 0.001$), yielded no reliable effects. Likewise, analysis of the ventral path ROIs found no effect of Strength on New targets (P's > 0.16; see Supplementary Fig. S1 for ROI time courses). (see Supplementary Material for additional exploratory brain–behavior analyses of univariate and connectivity measures along the ventral pathway.)

Effects of Memory Strength and Congruency Outside of the Ventral Path

To test the specificity of the controlled retrieval effect along the ventral path, we next tested ROIs outside of the hypothesized ventral retrieval pathway. First, we focused analysis on regions hypothesized to be related to postretrieval cognitive control, such as response selection. Specifically, we defined ROIs along a dorsal cognitive control pathway based on those previously implicated in a fronto-parietal control network (Table 1; "17-network parcellation" in Yeo et al. 2011). We also included mid-VLPFC in this group because: 1) it has been previously implicated in postretrieval control (Badre et al. 2005) and 2) it has been shown to correlate with this broader fronto-parietal network during resting-state connectivity analysis (Yeo et al. 2011).

In contrast to the main effect of Strength observed in the ventral path regions, none of the ROIs along this dorsal network demonstrated a main effect of Strength, and instead demonstrated the Strength × Congruency interaction predicted by the response selection hypothesis (Supplementary Fig. S3). Specifically, mid-VLPFC exhibited a Strength by Congruency interaction ($F_{1,18} = 9.3$, $P < 0.001$), without main effects of Strength or Congruency (F's < 2.2; P's > 0.05). A reliable Strength × Congruency interaction was also observed in PFC$_{lp}$ and IPS (PFClp: $F_{1,18} = 7.3$, $P < 0.05$; IPS: $F_{1,18} = 6.2$, $P < 0.05$), and a marginal effect on PFC$_{l}$ ($F_{1,18} = 3.2$, $P = 0.07$). A main effect of Strength was not observed in any of these ROIs (all P's > 0.70). When the Strength analysis was confined to the Incongruent case alone, the Strong > Weak effect was not reliable in any of the dorsal path ROIs, though there was a trend toward the effect in PFClp (all F's < 1.85, all P's > 0.08). The IPS and the 2 dorsal prefrontal ROIs showed a main effect of Congruency (F's$_{1,18}$ > 5.1, $P < 0.05$), such that there was overall greater activation for Congruent than Incongruent conditions (see Supplementary Material for a discussion of this main effect).

To summarize, we found that ROIs defined along the a priori ventral path consistently showed a main effect of Strength without an interaction with Congruency, whereas those defined in the more dorsal fronto-parietal control network consistently showed an interaction of Strength with Congruency. To confirm these observations at the network level, we next analyzed the a priori ROIs from each pathway (ventral: aVLPFC, aTC, aPHG, and HPC; dorsal: mid-VLPFC, PFCl, PFClp, and IPS), in separate ROI × Strength (Weak/Strong) × Congruency (Congruent/Incongruent) ANOVAs. Results from this analysis confirmed the functional differences between these 2 pathways (Fig. 4). Specifically, the ventral path ANOVA exhibited a main effect of Strength ($F_{1,18} = 5.4$, $P < 0.05$; Fig. 4*A*), as well as reliable

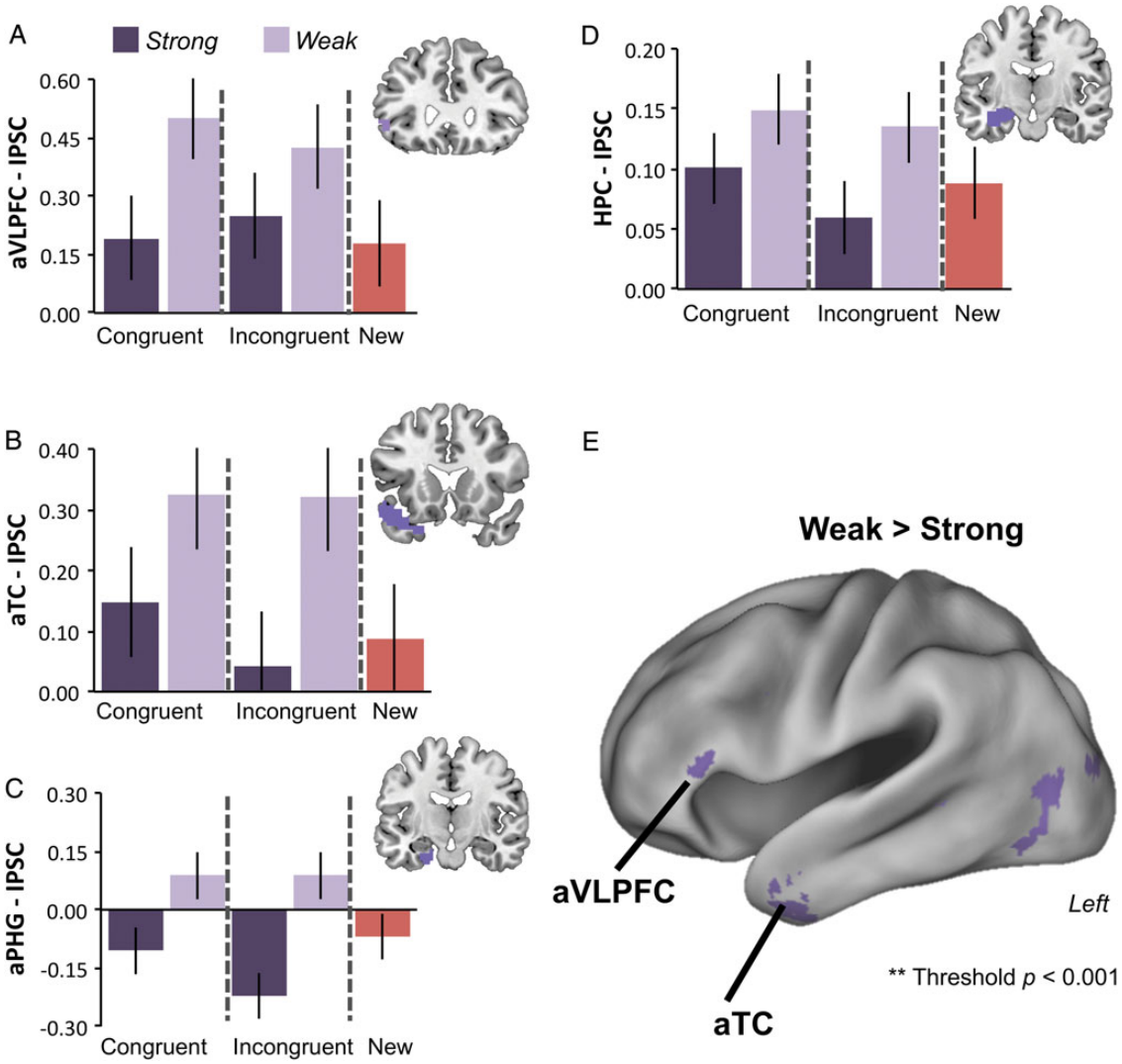

Figure 3. Effects of Strength and Congruency along the ventral pathway. Bars plot IPSC from the crossing of Strength and Congruency in the ROI analyses of the a priori ventral path regions: (*A*) aVLPFC, (*B*) aTC, (*C*) aPHG, and (*D*) HPC. Response to New items is also plotted for reference. In general, IPSC tracks Strength independently of Congruency in these regions consistent with a controlled retrieval process. Error bars depict within-subject standard error. (*E*) Surface rendering on the left hemisphere of the whole-brain voxelwise contrast of Weak > Strong ($P < 0.001$, uncorrected). This contrast shows that the effects of Strength are primarily in aVLPFC and temporal/ventral occipital cortex. The VLPFC activation cluster straddles the horizontal ramus of the lateral fissure, and so includes dorsal portions of BA47 and the rostral portion of BA45. Error bars depict within-subject standard error.

simple effects of Weak > Strong within each level of Congruency (Congruent: $t_{(1,18)} = 2.2$, $P < 0.05$; Incongruent: $t_{(1,18)} = 2.2$, $P < 0.05$). Notably, the effect of Weak over Strong within the Incongruent condition is a positive prediction of the controlled retrieval hypothesis. Response selection predicts the opposite effect (Strong > Weak Incongruent). Neither a main effect of Congruency nor a Strength × Congruency interaction were observed (all P's > 0.33).

In contrast, in the dorsal path ANOVA, there was no main effect of Strength in this pathway ($P > 0.45$). There was, however, the Strength by Congruency interaction ($F_{1,18} = 8.2$, $P < 0.01$; Fig. 4*B*) that is the prediction of the results selection hypothesis. There was a main effect of Congruency ($F_{1,18} = 5.2$, $P < 0.05$); Fig. 4*B*) in the dorsal path, such that Congruent conditions were more activated than Incongruent.

The Strength by Congruency interaction in the dorsal path regions provides support for the response selection hypothesis and distinguishes these regions from those of the ventral path. However, it is notable that Strong Incongruent activation was not consistently greater than Strong Congruent across the dorsal path ROIs, even appearing to show the reverse pattern quantitatively in some cases (see Supplementary Material for further discussion of this pattern of data). Thus, in order to further test the association of the dorsal path regions with response selection, we median split participants based on the magnitude of their Strong Incongruent versus Strong Congruent RT difference (we excluded the one participant whose RT difference was equal to the median). We then compared the difference in Strong Incongruent versus Strong Congruent activation between these groups. Consistent with a response selection hypothesis, this analysis revealed a reliable median split difference in dorsal path activation ($t_{(16)} = 2.2$, $P < 0.05$), as well as in mid-VLPFC activation specifically ($t_{(16)} = 2.3$, $P < 0.05$).

Finally, to confirm the functional dissociation between the dorsal and ventral pathways, we conducted a combined Path (Ventral/Dorsal) × Strength (Weak/Strong) × Congruency

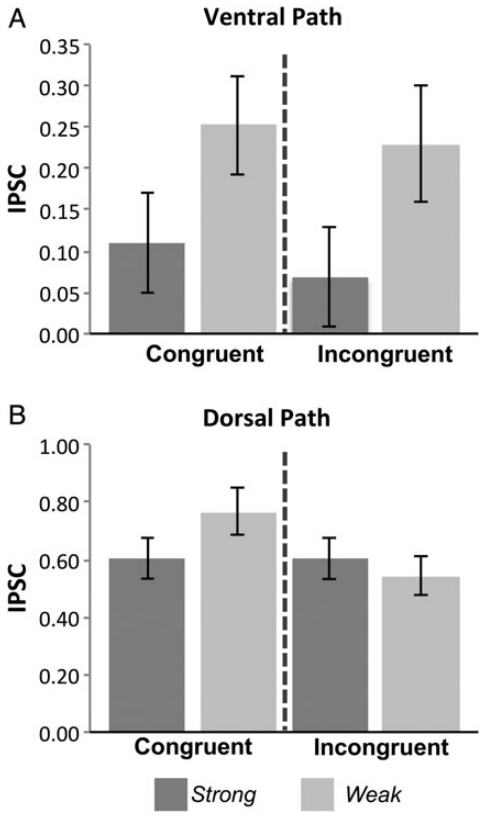

Figure 4. The ventral and dorsal pathways are involved in separable control processes. Activation in regions defined a priori along the ventral path (top) track the modulation of Strength rather than Congruency or the interaction of both factors. Importantly, significantly greater activation is observed for Weak than Strong within the Incongruent condition ($P < 0.05$), a pattern inconsistent with a response selection effect. In contrast, activation in regions defined a priori along the fronto-parietal "dorsal path" (bottom) reliably track the interaction of Strength and Congruency, implicating this pathway in postretrieval selection rather than memory access. Error bars depict within-subject standard error.

(Congruent/Incongruent) ANOVA. This analysis yielded a reliable Path × Strength × Congruency interaction ($F_{1,18} = 5.6$, $P < 0.05$). A further Path × Strength ANOVA within the diagnostic Incongruent condition confirmed the critical Path by Strength interaction predicted for this condition ($F_{1,18} = 12.3$, $P < 0.005$).

Given the potential partial overlap of the ventral path with the "default network" (Raichle et al. 2001; Greicius et al. 2003; Fox et al. 2005), we tested a set of ROIs outside the ventral path that are components of default network as defined by others (Yeo et al. 2011; Table 1). No ROI tested showed a main effect of Strength. Along the medial surface of PFC, dorsomedial PFC (PFC_{dm}, Table 1) showed greater activation for Incongruent relative to Congruent ($F_{1,18} = 5.5$, $P < 0.05$). No other regions tested showed reliable effects of Strength or Congruency.

Finally, to ensure that the selective effects of controlled retrieval observed along the ventral pathway were not driven by the restricted field of view entailed by our ROI approach, we conducted an exploratory whole-brain analysis at a lenient threshold conventionally used in the recognition memory literature ($P < 0.001$, uncorrected). Greater activation in left aVLPFC (−54 30 3), aTC (−48 6 −43), left mid-occipital (−45 −75 7), and bilaterial calcarine/lingual gyri (21 −72 −10; 18 −63 13; −15 −73 10) was observed in the whole-brain Weak > Strong contrast (Fig. 3*E*). No significant whole-brain effects were observed in the Strength by Congruency interaction.

Functional Connectivity Along the Ventral Path

The univariate analysis implicated the a priori-hypothesized regions along the ventral path in controlled retrieval. We next conducted functional connectivity analysis among these ROIs to test the hypothesis that these regions form a functional network. Figure 5 shows the pattern of whole-brain correlation ($P < 0.05$, FDR-corrected) within the Weak Source retrieval condition associated with each of the 4 a priori seeds along the ventral pathway (aVLPFC, aTC, aPHG, and HPC). These results provide initial evidence that these 4 ROIs do indeed affiliate as a network during source retrieval. However, not all 4 regions correlate equivalently with each other. Specifically, while aTC (Fig. 5, second from top) and HPC (Fig. 5, bottom) both correlated with all ventral path targets, the aVLPFC-seed network did not include aPHG (Fig. 5, second from bottom), and the aPHG-seed network included relatively few voxels from aVLPFC (Fig. 5, top). We did not observe reliable between Strength condition differences in network engagement in any of our seed regions. Thus, the following functional connectivity results are from the analysis of seed connectivity during Weak Source retrieval, when controlled retrieval demands are greatest, but similar results were also observed for Strong blocks.

Figure 6 (top, dark purple) shows the network formed from the conjunction ($P < 0.05$ FDR-corrected for valid "AND" conjunction) of the 4 individual network maps. The resulting network recovers 3 of the 4 a priori seed regions showing memory strength effects: aVLPFC, aTC, and HPC. In addition, the 4-way conjunction included lateral OFC, insula, and both anterior and posterior aspects of MTG.

The absence of aPHG from the 4-way conjunction network was likely due to weak aVLPFC-aPHG connectivity. To demonstrate this, we first conducted a conjunction analysis between aTC and HPC, as these seeds were robustly correlated with all ventral path seeds. The majority of voxels surpassing the valid conjunction threshold of $P < 0.05$ (FDR-corrected) closely followed the spatial topography of the left ventral path, including voxels in aVLPFC, aTC, aPHG, and HPC (Fig. 6, top light purple). The aTC–HPC conjunction also yielded a broader network than the restricted ventral path evident in the 4-way conjunction. Specifically, areas of convergence outside of the ventral path include mid cingulate cortex, striatum, and thalamus. We used this inclusive aTC-HPC conjunction as a reference definition of the ventral network.

Next, we examined how the aTC-HPC retrieval network changed by including aVLPFC versus aPHG in the conjunction respectively. The conjunction of the aVLPFC–seed network with the aTC-HPC network ("aVLPFC conjunction"; Fig. 6, second from top) yielded a more restricted, left lateralized functional network. Specifically, this conjunction included the a priori ventral path structures minus aPHG, along with a cluster spanning MTG terminating in a large cluster at the posterior extent of MTG (cMTG; see Supplementary Material (*e*) for additional analysis of cMTG). The aVLPFC conjunction network also included striatum and thalamus. The aPHG–Core conjunction network ("aPHG conjunction"; Fig. 6, second from bottom) did include voxels from all a priori seeds, including a small cluster in aVLPFC. Overall, frontal connectivity was

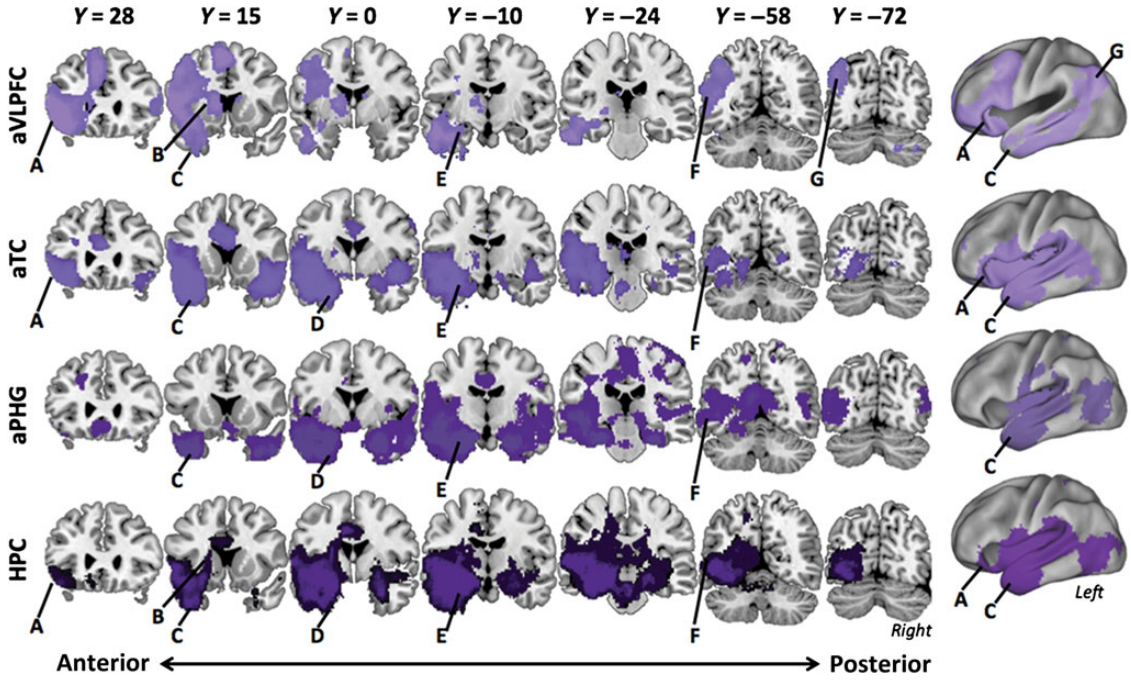

Figure 5. Functional connectivity along the ventral path during Source retrieval. Voxelwise connectivity of each of the 4 ventral path seeds (labels at left of each row) is plotted. Functional networks across Weak and Strong conditions were similar within each of these seeds, thus only the Weak Source condition is pictured. Major structures of interest are labeled: (*A*) aVLPFC, (*B*) striatum, (*C*) aTC, (*D*) aPHG, (*E*) HPC, (*F*) cMTG, (*G*) angular gyrus/IPS.

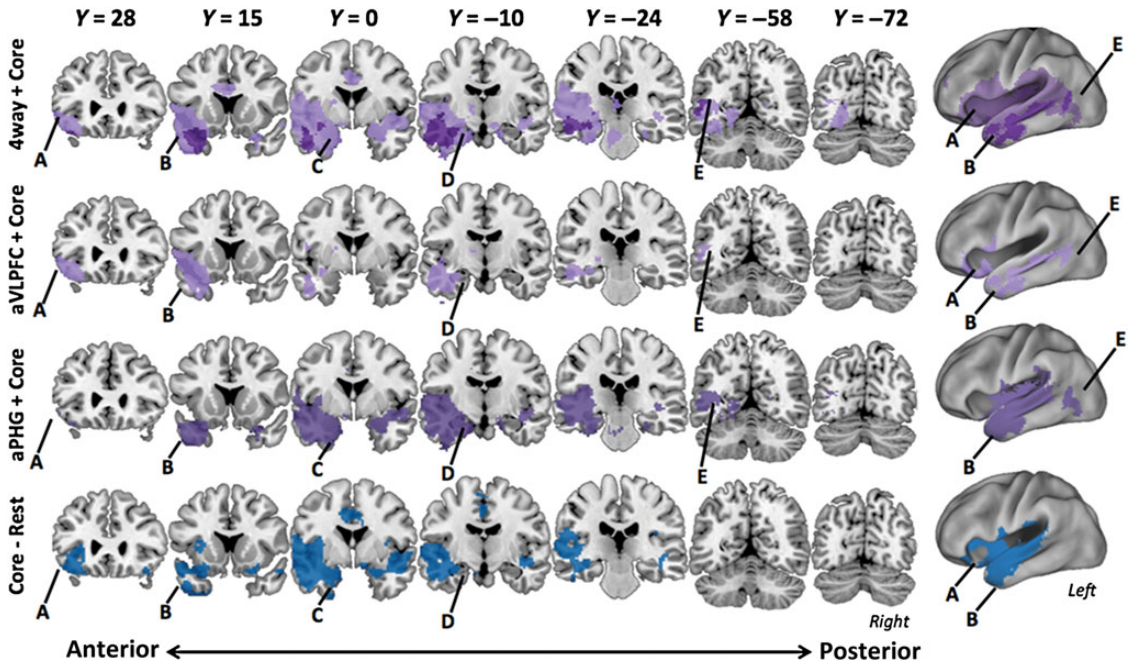

Figure 6. Conjunction analyses of connectivity along the ventral pathway. Voxelwise results from 4 connectivity analyses (labels at left of each row) are plotted on coronal slices. All contrasts are valid "AND" conjunctions from FDR-corrected seed maps thresholded at $P < 0.05$. Major structures of interest are labeled: (*A*) aVLPFC, (*B*) aTC, (*C*) aPHG, (*D*) HPC, and (*E*) cMTG. The top row plots conjunction analyses showing the most (light plot) and least (dark plot) inclusive definitions of the retrieval network. The aTC–HPC connectivity conjunction network is in light purple, and the more restricted the 4-way conjunction of the connectivity maps from the 4 a priori seeds is plotted in dark purple. The second and third rows depict the aVLPFC-conjunction in lilac (labeled "aVLPFC Conj.") and aPHG-conjunction in medium purple (labeled "aPHG Conj."), respectively. The bottom row (labeled "Core–rest") plots results of the aTC–HPC conjunction at rest in blue.

reduced in the aPHG conjunction and when compared with the aVLPFC conjunction network, and included more targets in posterior cortex. Also, in contrast to the pronounced left laterality of the aVLPFC conjunction (Fig. 6, second from top), connectivity with right hemisphere targets was stronger in the aPHG conjunction.

Connectivity Along the Ventral Fronto-Temporal Retrieval Pathway at Rest

The task-related effects of memory strength were specific to seeds that are part of the aTC–HPC network, suggesting that functional coupling within this network may be related to controlled retrieval. However, as these seeds respond similarly across task conditions, it is important to establish that their functional connectivity is not merely mediated by their comparable responses to task variables. To address this concern, we analyzed resting-state correlations among the seeds defined from our univariate analyses. As can be seen in Figure 6 (blue), reduced, but reliable, convergent connectivity was observed in a network encompassing approximately the same the network of regions identified by the task-based analysis.

Though reobtaining the network among ventral path regions at rest rules out an effect of task driving the effects we see in the task conditions, it remains open whether correlation among ventral path regions increases during the Source task. To test this, we compared the point-to-point correlations between aVLPFC and the 3 other ventral path ROIs from each memory Strength condition to aVLPFC–ventral path correlations at rest. Of these 6 tests, we found a reliable difference in the aVLPFC to HPC connectivity between Weak trials and rest ($t_{(17)} = 3.1$, $P < 0.05$ Bonferroni corrected). Other task-versus-rest comparisons were not significant (P's > 0.26). Thus, we did locate evidence for increased connectivity between PFC and MTL during the Weak strength trials of the source task relative to rest.

Differences in Functional Connectivity Among the Ventral Path ROIs

We next investigated the unique connectivity with aVLPFC and aPHG seeds that was distinct from the reference ventral network. This analysis suggested that aVLPFC differs from the other ventral path seeds in that it also connects with regions along the dorsal pathway. Specifically, we tested what regions in the aVLPFC and aPHG networks differed from the core aTC–HPC retrieval network by subtracting the aTC–HPC conjunction from the individual seeds separately ((aVLPFC Conjunction–(aTC ∩ HPC)) or (aPHG Conjunction–(aTC ∩ HPC)). Relative to the aTC–HPC network, aVLPFC correlated substantially with mid-VLPFC, DLPFC (~BA 46), and angular gyrus. Subcortically, aVLPFC also correlated more with basal ganglia and thalamus. In contrast to aVLPFC, functional connectivity of aPHG was reduced, but similar to the aTC–HPC network.

Specificity of the Ventral Path Network for Retrieval

To confirm the functional specificity of ventral path recruitment by our a priori seeds, we next examined the functional networks associated with seed regions outside the ventral path that showed reliable task-related activation, but not the specific controlled retrieval pattern. We assessed the extent to which these networks included regions along the a priori ventral path.

First, we assessed the functional connectivity of mid-VLPFC, the seed that tracked the univariate Strength × Congruency interaction (Supplementary Fig. S3). Mid-VLPFC functionally coupled with a network comprised of voxels mainly in the dorsolateral frontal and inferior parietal lobes, as well as with ITG and the basal ganglia (Fig. 7. top). Evidence of overlap between structures functionally connected with the mid-VLPFC and the 4-way conjunction network was largely absent from with the crucial exception of aVLPFC, a member of both networks (Fig. 7, bottom). Moreover, there was considerable overlap between mid-VLPFC and the aVLPFC network especially in DLPFC and parietal cortex (Fig. 7, middle). Indeed, the primary difference between aVLPFC and mid-VLPFC was the unique functional coupling of aVLPFC with the ventral path (Fig. 7, bottom). Conversely, the sole site of overlap between the mid-VLPFC network and the 4-way conjunction retrieval network was aVLPFC and cMTG.

Finally, we compared the functional connectivity of our exploratory ROIs from the default and fronto-parietal control systems (Yeo et al. 2011) with the connectivity pattern of the

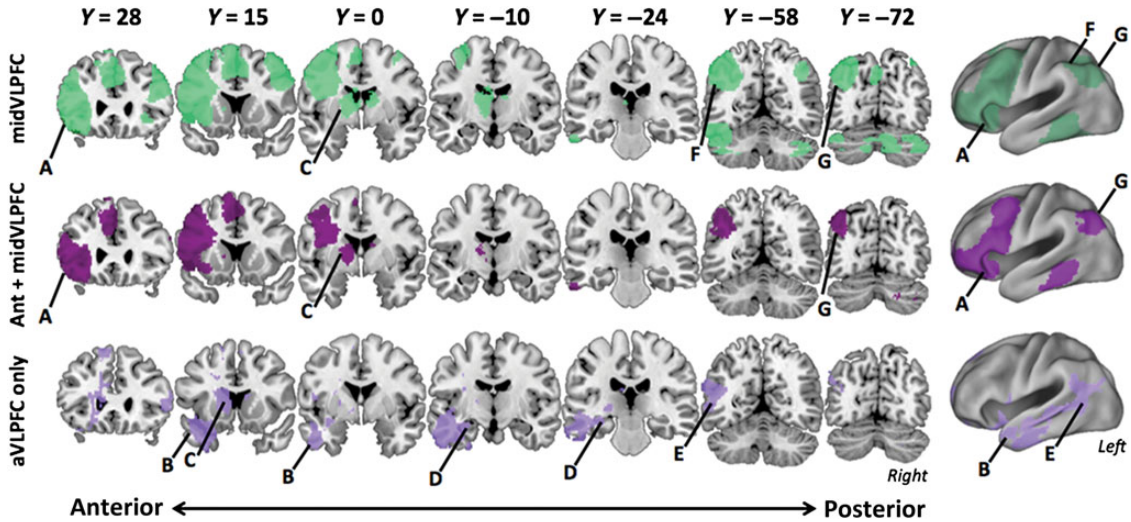

Figure 7. Analyses of specificity of the ventral path network. (*A*) Voxelwise results from the functional connectivity analysis of the mid-VLPFC seed are plotted in green. Mid-VLPFC includes mostly dorsal frontal-parietal sites with aVLPFC being the only ventral path region in its network (<10 voxels, (*A*). AVLPFC and mid-VLPFC also share voxels in mid-caudal MTG, but shared voxels are sparse and are not easily visualized. (*B*) The conjunction ($P < 0.05$ FDR) of the mid-VLPFC and aVLPFC connectivity maps reveals overlap among the dorsolateral PFC and parietal components of the aVLPFC network (maroon). (*C*) The subtraction of the connectivity map of mid-VLPFC from aVLPFC reveals regions of the ventral retrieval network plotted in lilac.

ventral retrieval pathway. Overlap between the conjunction of the default network seeds and the ventral retrieval pathway is minimal (8, top and bottom), although we should note that we are using a comparatively restricted definition of the default network ("17-network parcellation," Yeo et al. 2011). The overlap between the ventral retrieval pathway and the fronto-parietal control seed networks was also limited (Fig. 8, middle).

Discussion

We provide novel evidence for a ventral polysynaptic pathway supporting PFC–MTL interactions during controlled episodic retrieval. First, regions hypothesized to be on the ventral path were distinguished from other task-active regions by their sensitivity to controlled retrieval, evident in an effect of memory Strength independent of Congruency. Next, the functional network common to these regions selectively encompassed the a priori ventral pathway seeds. More specifically, we showed: 1) regions along the ventral path exhibited a "small world" quality in that each of these seeds recovered the other seeds in its network. 2) A similar network could be recovered in the absence of third variable effects of a retrieval task (i.e., at rest). 3) Only aVLPFC included other networks (specifically the dorsal fronto-parietal control network) in its unique connectivity pattern. And 4), of the ventral path regions, only aVLPFC was included in the functional networks of regions defined along the dorsal pathway, here associated with response selection demands. We now consider these findings in greater detail.

The 4 regions defining the ventral pathway are consistent with prior anatomical and connectivity studies identifying

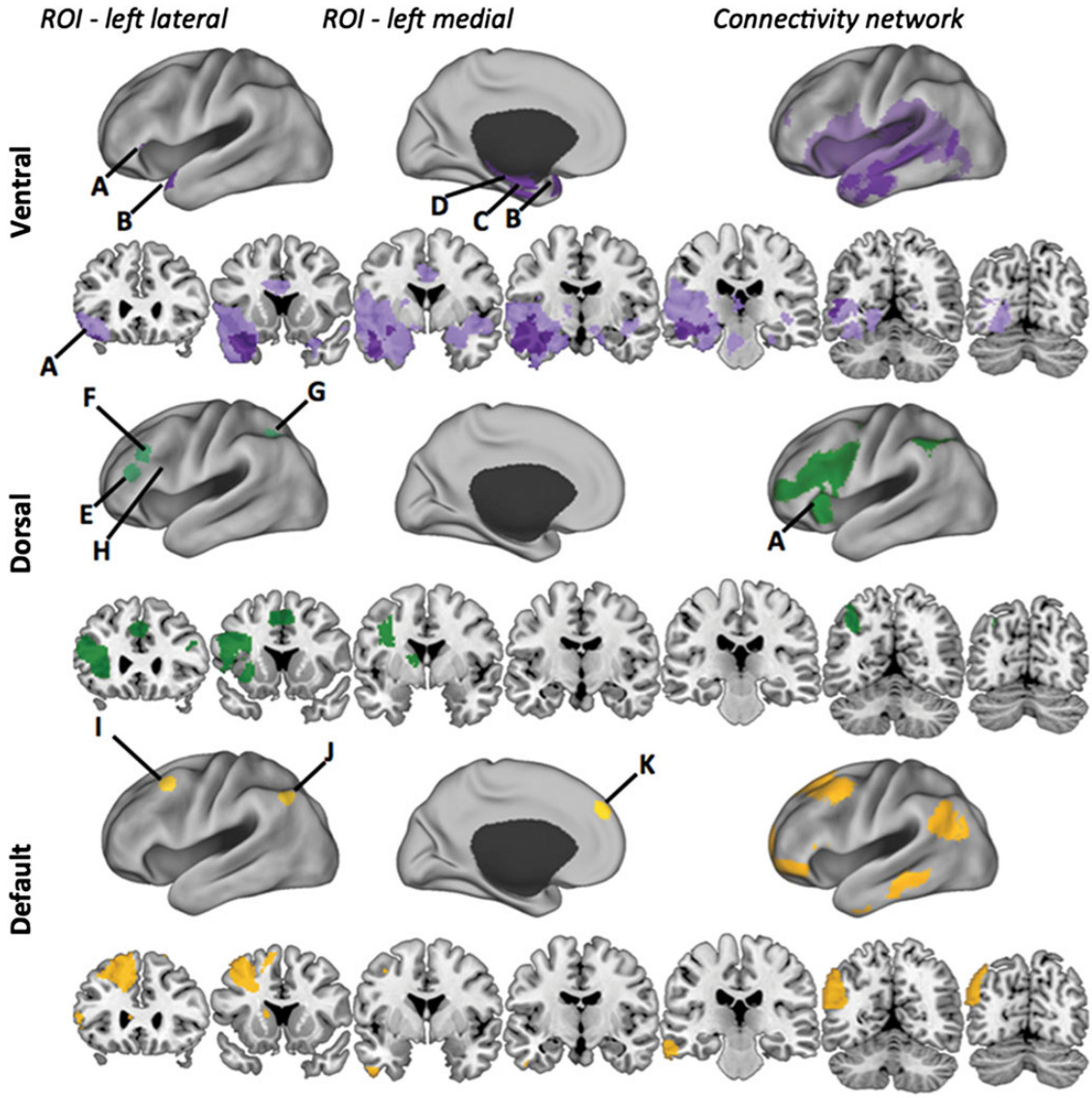

Figure 8. Comparison of default and fronto-parietal control network seeds to the retrieval network. The ventral path connectivity network is plotted in purple (top), with the lighter shade denoting the Core connectivity network and the darker the 4-way conjunction. ROIs are defining ventral path network are marked and include (*A*) aVLPFC, (*B*) aTC, (*C*) aPHG, and (*D*) HPC. The dorsal network is plotted in green (middle). The fronto-parietal ROIs are marked and include (*E*) PFC_{l}, (*F*) PFC_{lp}, (*G*) IPS, and (*H*) mid-VLPFC. Note that mid-VLPFC lies within the sulcus and cannot be seen in lateral view; approximate location only is marked. The conjunction of the networks generated from 3 a priori default network seeds, (*I*) PFC_{dp}, (*J*) PGp_{d}, and (*K*) PFC_{dm}, are plotted in yellow (bottom). Comparison across networks illustrates that the overlap between fronto-parietal control network and retrieval network is primarily limited to aVLPFC. The retrieval network overlaps with the ventral portion of the default network.

connections among these regions (Eberling and von Cramon 1992; Kier et al. 2004; Thiebaut de Schotten et al. 2012). However, the present study indicates that these regions may operate together as a polysynaptic pathway supporting controlled retrieval. Moreover, 2 previous studies combined fMRI and diffusion tensor imaging to reconstruct tracts from ROIs in PFC active during memory encoding and item recognition to temporal lobe structures (Takahashi et al. 2007; Schott, Niklas et al. 2011). In both studies, tracts from PFC subregions to MTL were reconstructed along a path approximating the ventral pathway located in the present experiment (though other pathways may also be critical for control at encoding, e.g., Cohen 2011). Likewise, beyond item recognition, a recent study found evidence of increased VLPFC–HPC coupling at encoding that was predictive of later free recall (Schott, Wüstenberg et al. 2011). The consistency of this pathway across encoding and retrieval strengthens the conclusion that the ventral pathway is a functional-anatomical circuit supporting PFC–MTL interactions during memory.

Though we associate the ventral path regions with controlled retrieval demands in the current study, our results should not necessarily be interpreted as indicating that the entire ventral pathway serves a uniform function. Rather, our hypothesis is that controlled retrieval is supported by dynamics in this network, whereby control signals originating in aVLPFC modulate the retrieval of task-relevant information from long-term memory stores in the posterior cortical regions. Thus, from this perspective, aVLPFC supports retrieval when control is required, whereas the other regions in the network support the storage and retrieval of long-term memories more generally, whether controlled or automatic. Correspondingly, we would predict that the univariate response in aVLPFC would only be driven by changes in demands for controlled retrieval, whereas the rest of the pathway would vary with demands on overall retrieval. Thus, it would be possible to dissociate aVLPFC from the rest of the ventral network, if the levels of automatic and controlled retrieval were independently varied across conditions.

Though we do not have such a manipulation in the current design, prior research on semantic retrieval has employed this logic to dissociate aVLPFC from posterior neocortical regions. For example, Badre et al. (2005) crossed a manipulation of controlled retrieval, using cue-target associative strength, with a manipulation of overall retrieval by varying number of word targets to be considered during a semantic decision. This latter "number-of-targets" manipulation required greater retrieval (recovering semantic details about each target) without necessarily impacting demands on controlled retrieval. Thus, crossing these manipulations permitted aVLPFC responses to controlled retrieval to be dissociated from those related to overall semantic retrieval in posterior lateral temporal cortex. We would predict a similar dissociation among ventral path regions, given an analogous manipulation of overall episodic retrieval.

Though more speculative, the specific contribution of aVLPFC in controlled, as opposed to overall retrieval, may also relate to its putative role as a hub linking between the ventral and dorsal networks. For example, engagement of this region during retrieval might provide a signal to postretrieval control mechanisms regarding deployment of "front-end" retrieval control signals. Such signals could be useful in modulating postretrieval mechanisms, or indeed, setting up expectations about the likely products of retrieval for monitoring systems. Understanding this observation will be an important goal for future research.

Following from the above discussion, it is also important to note that the present correlations cannot provide evidence of direction of influence along the ventral pathway. Though we have discussed the ventral path as a fully feedforward system, it is conceivable that, in the service of controlled retrieval, aVLPFC and temporal lobe regions could share feedforward, feedback, or complex bidirectional interactions that are modulated as a function of retrieval demand. Characterizing these aVLPFC-temporal lobe interactions, while incorporating regions both within and outside of the ventral pathway, will be an important direction for future research.

In contrast to ventral path regions, regions of DLPFC and IPS connected in a distinct dorsal fronto-parietal network, consistent with prior observations (Dosenbach et al. 2007; Vincent et al. 2008; Yeo et al. 2011). Only aVLPFC among ventral path regions correlated with this network. These dorsal fronto-parietal regions were further distinguished from the ventral path in that their univariate response tracked the Strength × Congruency interaction, implicating this network in response selection processes. Intriguingly, mid-VLPFC demonstrated a similar Strength × Congruency interaction and correlated with regions of the dorsal fronto-parietal system but not ventral path regions beyond aVLPFC. Importantly, different univariate responses to Strength and Congruency supported a functional dissociation between these 2 pathways.

Following from the above observations, the present results extend current theory regarding the functional contributions of left VLPFC to the cognitive control of memory retrieval. Prior work has reported functional dissociations between aVLPFC and mid-VLPFC related to controlled retrieval and postretrieval selection, respectively (Badre et al. 2005). While this dissociation was observed in the semantic memory domain, the present results from an episodic retrieval task are consistent with this distinction and extend it to 2 broader functional networks.

The main effect of Strength in aVLPFC, independent of Congruency, is consistent with the hypothesis that aVLPFC biases retrieval of semantic representations in temporal cortex in the service of controlled retrieval. This elaborative process shapes the input to MTL, thereby influencing pattern completion and ultimately increasing the probability that task-relevant memories are retrieved. Moreover, as discussed already, the unique correlation of aVLPFC with both the ventral path and the dorsal fronto-parietal network extends the role of this region to that of a potential "hub" between these functionally distinct networks.

Mid-VLPFC, in contrast, was sensitive to the interaction of Strength and Congruency implicating this region in response selection processes. Incongruent trials require participants to reject an item that was encountered previously. As evidence of oldness may drive a yes response, rejecting these Incongruent items should tax processes required to select the appropriate response in the face of competition (here, arising from conflict between the yes and no responses).

Importantly, however, though we have discussed this demand as a motor or action-level control process, it is possible that this pattern could emerge at a decision or monitoring level. Consider that Incongruent trials result not only in conflicting response tendencies but also conflicting evidence. For example, familiarity or nondiagnostic recollection details may

be evidence for a "yes" response, whereas diagnostic recollected details could be evidence for a "no" response. Thus, this ambiguity might also tax decision processes that set criteria and thresholds or monitor retrieved information for its relevance to current decision criteria. These mechanisms would all qualify as postretrieval in that they operate on the products of retrieval rather than influencing access itself (Badre and Wagner 2007; Benjamin 2007), and so are consistent with the basic functional dissociation between the ventral and dorsal pathways. However, the present design is not able to further specify the nature and level of these processes. And indeed, prior work has focused on mid-VLPFC, for example, in selection of relevant retrieved information, as opposed to motor response selection, per se.

Beyond these functional differences, network-level connectivity clearly differentiated aVLPFC and mid-VLPFC (Fig. 8), wherein mid-VLPFC was exclusively associated with the dorsal fronto-parietal network. Hence, these results place functional distinctions between aVLPFC and mid-VLPFC within the context of their broader functional networks. Most notably, prior work has used the term VLPFC interchangeably with the inferior frontal gyrus, leading to functional anatomic distinctions being tested within this bounded anatomical region. However, the present data indicate that the inferior frontal sulcus may not be a meaningful functional boundary. Rather, prior definitions of mid-VLPFC may have mixed the ventral extension of the dorsal fronto-parietal network with a portion of the ventral path. In contrast, prior definitions of aVLPFC are more likely to have fallen entirely within the ventral path network. It follows, then, that previous functional distinctions between aVLPFC and mid-VLPFC observed in fMRI may partly reflect the differential contributions of these separate functional networks.

Beyond the cortico-cortical ventral pathway, other pathways connecting aVLPFC and MTL may also be consistent with our present results. In this regard, it was notable that aPHG was not in the network generated from the aVLPFC seed. To some degree, this null result likely reflects sensitivity or power, as the converse analysis, seeding aPHG, reliably correlated with voxels in aVLPFC. Nevertheless, the relatively weak relationship between aPHG and aVLPFC merits consideration given the robust connectivity of aVLPFC with HPC, an interaction that should theoretically be mediated by aPHG in a strict feedforward model. One account of this pattern is that it reflects the convergence of several pathways between aVLPFC and HPC.

One such pathway could rely on interactions with the basal ganglia. The basal ganglia may contribute to memory encoding (Lisman and Grace 2005; Shohamy and Adcock 2010) and retrieval (Han et al. 2010; Scimeca and Badre 2012; Schwarze et al. 2013), and share anatomical connections with ventral path regions (Whitlock and Nauta 1956; Yeterian and Pandya 1991; Thierry et al. 2000; Furtak et al. 2007; Leh et al. 2007). In our data, the HPC and aVLPFC seeds each correlated reliably with striatum, whereas the aPHG seed did not (Fig. 5). Consequently, the strong aVLPFC-HPC correlations, in the presence of weak connectivity between aPHG and aVLPFC, could partially emerge from convergent input from a basal ganglia mediated pathway. Other paths capable of supporting aVLPFC-HPC interactions could arise via aVLPFC connections with orbital PFC, DLPFC, or the cingulum bundle.

As a final point, we did not observe reliable condition differences in connectivity along the ventral path, despite the clear univariate effects (though see Supplementary Material brain–behavior analysis). However, one should be cautious about interpreting this null result, as the functional significance of univariate and multivariate effects in terms of underlying neural dynamics is still an open issue; there are as yet no agreed upon biophysical models that relate neural activity to both univariate BOLD responses and BOLD correlation between regions (though see Friston 2011; O'Reilly et al. 2012). Indeed, there are several plausible task-related neural dynamics within a connected network of which an over additive increase in neural firing and coherence is only one. Moreover, it is possible that blocking of Strength may have introduced noise (such as through the inclusion of error trials) that reduces our sensitivity to detect conditions differences in connectivity. Nevertheless, the pattern of univariate and multivariate effects observed here may suggest that cognitive control along the ventral path is largely instantiated in terms of the content of neural representations in regions along the ventral path (affecting only regional cellular metabolism), rather than dynamic changes in the degree of coherence among these neural populations.

The present results may also inform recent debates regarding the role of posterior parietal cortex in memory retrieval. The posterior parietal cortex is functionally heterogeneous, with functional differences being commonly noted between dorsal versus ventral parietal cortex (Wagner et al. 2005; Rugg and Curran 2007; Cabeza et al. 2008; Ciaramelli et al. 2008; Vilberg and Rugg 2008), and recent work providing evidence for finer subdivisions (Hutchinson et al. 2009, 2012; Nelson et al. 2010; Sestieri et al. 2010). Two observations from the present study may inform this literature.

First, though the angular gyrus has been implicated in memory, it was not consistently correlated with the regions along the ventral pathway. This result appears consistent with a recent study (Burianová et al. 2012) reporting that right inferior frontal gyrus and left posterior parahippocampal gyrus, among other regions were correlates of ventral parietal cortex, but excluded the full ventral path as defined here.

Notably, however, while the ventral path as a whole was not correlated with angular gyrus, angular gyrus was included in the aVLPFC-seed network. This seems in line with recent accounts tying angular gyrus to bottom up attention-to-memory (Cabeza et al. 2012). For example, such a mechanism could play a role in eliciting controlled retrieval, which we attribute to aVLPFC here, reactively. This correlation with aVLPFC could also be consistent with other accounts of angular gyrus function related to episodic output and integration (Wagner et al. 2005; Vilberg and Rugg 2008). However though angular gyrus specifically correlated with aVLPFC, supramarginal gyrus was correlated with all 4 regions of the ventral path. Thus, the functional heterogeneity of ventral path connectivity with parietal cortex complicates drawing strong conclusions about the functional significance of the present results.

In dorsal parietal, IPS correlated with other members of the dorsal fronto-parietal network, consistent with previous studies (Yeo et al. 2011; Burianová et al. 2012). Prior work provides an anatomical basis for fronto-parietal connections underlying this network. In particular, human tractography (Rushworth et al. 2006; Frey et al. 2008; Caspers et al. 2011; Thiebaut de Schotten et al. 2012), combined dissection/tractography (Martino et al. 2011), and tracers in nonhuman primates (Goldman-Rakic and Schwartz 1982; Petrides and

Pandya 2009) have shown that frontal areas, in both DLPFC and posterior VLPFC are connected with parietal cortex by association fibers, such as those of the superior longitudinal fasciculus. However, it should be noted that the IPS is a heterogeneous region and prior work has shown that subregions of IPS can participate in different networks (Uddin et al. 2010). For example, IPS1 and IPS2 are functionally connected with frontal cortex, whereas IPS3 is preferentially connected to higher-level visual areas. The IPS ROI used in the present study encompasses portions of IPS1 and IPS3. And, indeed, its network shares features of both the IPS1 and IPS3 networks defined in Uddin et al. (2010). Thus, in the absence of precise anatomical data (such as from diffusion tractography), we cannot be certain about which IPS subregions contribute to the IPS seed network observed here or their mapping to the univariate effects we observe.

Notwithstanding the above caveat regarding its precise locus, IPS showed an interaction between Strength and Congruency, akin to other regions in the dorsal network. This observation builds on recent work identifying memory strength effects in IPS (Hutchinson et al. 2012). That study concluded that though IPS tracked perceived memory strength, its activation may reflect an accumulation-based decision making process. Using a different operational definition of memory strength, the present results support this conclusion by demonstrating that strength alone does not drive IPS, but IPS responds in accord with the way that strength interacts with a decision.

In conclusion, these results provide novel evidence of a functional VLPFC-MTL pathway involved in the controlled episodic retrieval. Moreover, observed differences in network-level connectivity differentiating aVLPFC and mid-VLPFC provide further support for functional distinctions drawn between VLPFC subregions contributing to the cognitive control of memory retrieval, and specify that previously observed differences reflect the differential contributions of separate ventral and dorsal functional networks to retrieval performance. Specifically, whereas the ventral pathway may support controlling memory access, such as by influencing the input to the memory system, the dorsal pathway may relate the products of retrieval to behavior, such as by controlling the output of the memory system.

Supplementary Material

Supplementary material can be found at: http://www.cercor.oxfordjournals.org/.

Funding

The present work was supported by an NIMH NRSA awarded to J.B. (1 F31 MH090755-01A1), an NINDS R01 (NS065046), and fellowships from the Alfred P. Sloan Foundation (BR2011-010) and the James S. McDonnell Foundation awarded to D.B.

Notes

We are grateful to P. Shih for help with connectivity analysis during the early stages of this project. We also thank C. Gorrostieta and H. Ombao for assistance with data analysis during early instantiations of this project. Finally, we wish to thank J. Scimeca, E. Nyhus, C. Chatham, and the rest of the Badre Lab for insightful comments during the preparation of this manuscript. *Conflict of Interest:* None declared.

References

Badre D, Poldrack R, Paré-Blagoev EJ, Insler RZ, Wagner AD. 2005. Dissociable controlled retrieval and generalized selection mechanisms in ventrolateral prefrontal cortex. Neuron. 47(6): 907–918.

Badre D, Wagner AD. 2006. Computational and neurobiological mechanisms underlying cognitive flexibility.Proc Natl Acad Sci U S A. 103(18):7186–7191.

Badre D, Wagner AD. 2007. Left ventrolateral prefrontal cortex and the cognitive control of memory. Neuropsychologia. 45(13): 2883–2901.

Benjamin AS. 2007. Memory is more than just remembering: strategic control of encoding, accessing memory, and making decisions. In: Benjamin AS, Ross BH, editors. The psychology of learning and motivation: skill and strategy in memory use. Vol. 48. London: Academic Press. p. 1–71.

Blaizot X, Mansilla F, Insausti AM, Constans JM, Salinas-Alamán A, Pró-Sistiaga P, Mohedano-Moriano A, Insausti R. 2010. The human parahippocampal region: I. Temporal pole cytoarchitectonic and MRI correlation. Cereb Cortex. 20(9):2198–2212.

Burianová H, Ciaramelli E, Grady CL, Moscovitch M. 2012. Top-down and bottom-up attention-to-memory: mapping functional connectivity in two distinct networks that underlie cued and uncued recognition memory. NeuroImage. 63(3):1343–1352.

Burwell RD, Agster KL. 2008. Anatomy of the hippocampus and the declarative memory system. In Eichenbaum HE (Ed.), Systems and Neuroscience (Vol. 3, pp. 47–66) of Byrne JH (Ed.), Learning and Memory: A Comprehensive Reference. Oxford: Elsevier.

Cabeza R, Ciaramelli E, Moscovitch M. 2012. Cognitive contributions of the ventral parietal cortex: an integrative theoretical account.Trends Cogn Sci. 16(6):338–352.

Cabeza R, Ciaramelli E, Olson IR, Moscovitch M. 2008. The parietal cortex and episodic memory: an attentional account. Nat Rev Neurosci. 9(8):613–625.

Caspers S, Geyer S, Schleicher A, Mohlberg H, Amunts K, Zilles K. 2006. The human inferior parietal cortex: cytoarchitectonic parcellation and interindividual variability. NeuroImage. 33(2):430–448.

Caspers S, Eickhoff SB, Geyer S, Scheperjans F, Mohlberg H, Zilles K, Amunts K. 2008. The human inferior parietal cortex in stereotaxic space. Brain Struct Funct. 212(6):481–495.

Caspers S, Eickhoff SB, Rick T, Von Kapri A, Kuhlen T, Huang R, Shah NJ, Zilles K. 2011. Probabilistic fibre tract analysis of cytoarchitectonically defined human inferior parietal lobule areas reveals similarities to macaques. NeuroImage. 58(2):362–380.

Ciaramelli E, Grady CL, Moscovitch M. 2008. Top-down and bottom-up attention to memory: a hypothesis (AtoM) on the role of the posterior parietal cortex in memory retrieval. Neuropsychologia. 46 (7):1828–1851.

Cohen MX. 2011. Hippocampal-prefrontal connectivity predicts midfrontal oscillations and long-term memory performance. Curr Biol. 21(22):1900–1905.

Dale AM. 1999. Optimal experimental design for event-related fMRI. Hum Brain Mapp. 8(2):109–114.

Dobbins IG, Foley H, Schacter DL, Wagner AD. 2002. Executive control during episodic retrieval: multiple prefrontal processes subserve source memory. Neuron. 35(5):989–996.

Dobbins IG, Rice HJ, Wagner AD, Schacter DL. 2003. Memory orientation and success: Separable neurocognitive components underlying episodic recognition. Neuropsychologia. 41(3):318–333.

Dobbins IG, Wagner AD. 2005. Domain-general and domain-sensitive prefrontal mechanisms for recollecting events and detecting novelty. Cereb Cortex. 15(11):1768–1778.

Dobbins IG, Han S. 2006. Isolating rule- versus evidence-based prefrontal activity during episodic and lexical discrimination: a functional magnetic resonance imaging investigation of detection theory distinctions. Cereb Cortex. 16(11):1614–1622.

Dosenbach NUF, Fair DA, Miezin FM, Cohen AL, Wenger KK, Dosenbach RAT, Fox MD, Snyder AZ, Vincent JL, Raichle ME et al. 2007. Distinct brain networks for adaptive and stable task control in humans. Proc Natl Acad Sci USA. 104(26):11073–8.
Eberling U, von Cramon D. 1992. Topography of the uncinate fascicle and adjacent temporal fiber tracts. Acta Neurochir. 115:143–148.
Fletcher PC, Henson RN. 2001. Frontal lobes and human memory: insights from functional neuroimaging. Brain. 124(5):849–881.
Fox MD, Snyder AZ, Vincent JL, Corbetta M, Van Essen DC, Raichle ME. 2005. The human brain is intrinsically organized into dynamic, anticorrelated functional networks. Proc Natl Acad Sci USA. 102 (27):9673–9678.
Frey S, Campbell JSW, Pike GB, Petrides M. 2008. Dissociating the human language pathways with high angular resolution diffusion fiber tractography. J Neurosci. 28(45):11435–11444.
Friston KJ. 2011. Functional and effective connectivity: a review. Brain Connect. 1(1):13–36.
Furtak SC, Wei S, Agster KL, Burwell RD. 2007. Functional neuroanatomy of the parahippocampal region in the rat: the perirhinal and postrhinal cortices. Hippocampus. 722:709–722.
Gold BT, Balota DA, Jones SJ, Powell DK, Smith CD, Andersen AH. 2006. Dissociation of automatic and strategic lexical-semantics: functional magnetic resonance imaging evidence for differing roles of multiple frontotemporal regions. J Neurosci. 26 (24):6523–6532.
Goldman-Rakic PS, Schwartz ML. 1982. Interdigitation of contralateral and ipsilateral columnar projections to frontal association cortex in primates. Science. 216(4547):755–757.
Greicius MD, Krasnow B, Reiss AL, Menon V. 2003. Functional connectivity in the resting brain: a network analysis of the default mode hypothesis. Proc Natl Acad Sci USA. 100(1):253–258.
Han S, Huettel SA, Raposo A, Adcock RA, Dobbins IG. 2010. Functional significance of striatal responses during episodic decisions: recovery or goal attainment? J Neurosci. 30(13):4767–4775.
Han S, O'Connor AR, Eslick AN, Dobbins IG. 2012. The role of left ventrolateral prefrontal cortex during episodic decisions: semantic elaboration or resolution of episodic interference? J Cogn Neurosci. 24(1):223–234.
Hayama HR, Rugg MD. 2009. Right dorsolateral prefrontal cortex is engaged during post-retrieval processing of both episodic and semantic information. Neuropsychologia. 47(12):2409–2416.
Hutchinson JB, Uncapher MR, Wagner AD. 2009. Posterior parietal cortex and episodic retrieval: convergent and divergent effects of attention and memory. Learn Mem. 650:343–356.
Hutchinson JB, Uncapher MR, Weiner KS, Bressler DW, Silver MA, Preston AR, Wagner AD. 2012. Functional heterogeneity in posterior parietal cortex across attention and episodic memory retrieval. Cereb Cortex. 1–18 [Epub ahead of print].
Jacoby LL. 1991. A process dissociation framework: separating automatic from intentional uses of memory. J Mem Lang. 30 (5):513–541.
Jetter W, Poser U, Freeman RB, Markowitsch HJ. 1986. A verbal long term memory deficit in frontal lobe damaged patients. Cortex. 22:229–242.
Janowsky JS, Shimamura AP, Kritchevsky M, Squire LR. 1989. Cognitive impairment following frontal lobe damage and its relevance to human amnesia. Behav Neurosci. 103:548–560.
Kahn I, Andrews-Hanna JR, Vincent JL, Snyder AZ, Buckner RL. 2008. Distinct cortical anatomy linked to subregions of the medial temporal lobe revealed by intrinsic functional connectivity. J Neurophysiol. 100(1):129–139.
Kier EL, Staib LH, Davis LM, Bronen RA. 2004. MR Imaging of the temporal stem: anatomic dissection tractography of the uncinate fasciculus, inferior occipitofrontal fasciculus, and Meyer's loop of the optic radiation. AJNR Am J Neuroradiol. 25:677–691.
Kucera H, Francis WN. 1967. Computational analysis of present-day English. Providence (RI): Brown University Press.
Leh SE, Ptito A, Chakravarty MM, Strafella AP. 2007. Fronto-striatal connections in the human brain: a probabilistic diffusion tractography study. Neurosci Lett. 419(2):113–118.
Lisman JE, Grace AA. 2005. The hippocampal-VTA loop: controlling the entry of information into long-term memory. Neuron. 46(5): 703–713.
Maril A, Simons JS, Mitchell JP, Schwartz BL, Schacter DL. 2003. Feeling-of-knowing in episodic memory: an event-related fMRI study. NeuroImage. 18:827–836.
Martino J, De Witt Hamer PC, Vergani F, Brogna C, De Lucas EM, Vázquez-Barquero A, García-Porrero JA, Duffau H. 2011. Cortex-sparing fiber dissection: an improved method for the study of white matter anatomy in the human brain. J Anat. 219(4):531–541.
McElree B, Dolan PO, Jacoby LL. 1999. Isolating the contributions of familiarity and source information in item recognition: a time-course analysis. J Exp Psychol Learn Mem Cogn. 25:563–582.
Moscovitch M. 1994. Cognitive resources and dual-task interference effects at retrieval in normal people: the role of the frontal lobes in medial temporal cortex. Neuropsychology. 8:524–534.
Nelson SM, Cohen AL, Power JD, Wig GS, Miezin FM, Wheeler ME, Velanova K, Donaldson DI, Phillips JS, Schlaggar BL et al. 2010. A parcellation scheme for human left lateral parietal cortex. Neuron. 67(1):156–170.
Nichols T, Brett M, Andersson J, Wager T, Poline J. 2005. Valid conjunction inference with the minimum statistic. NeuroImage. 25(3): 653–660.
O'Reilly JX, Woolrich MW, Behrens TEJ, Smith SM, Johansen-Berg H. 2012. Tools of the trade: psychophysiological interactions and functional connectivity. Soc Cogn Affect Neur. 7(5):604–609.
Öztekin I, Badre D. 2011. Distributed patterns of brain activity that lead to forgetting. Frontiers Hum Neurosci. 5(86):1–8.
Petrides M, Pandya DN. 2001. Comparative cytoarchitectonic analysis of the human and the macaque ventrolateral prefrontal cortex and corticocortical connection patterns in the monkey. Eur J Neurosci. 16(2):291–310.
Petrides M, Pandya DN. 2009. Distinct parietal and temporal pathways to the homologues of Broca's area in the monkey. PLoS Biol. 7(8): e1000170.
Petrides M, Tomaiuolo F, Yeterian EH, Pandya DN. 2012. The prefrontal cortex: comparative architectonic organization in the human and the macaque monkey brains. Cortex. 48(1):46–57.
Race EA, Shanker S, Wagner AD. 2009. Neural priming in human frontal cortex: multiple forms of learning reduce demands on the prefrontal executive system. J Cogn Neurosci. 21(9):1766–1781.
Raichle ME, MacLeod AM, Snyder AZ, Powers WJ, Gusnard DA, Shulman GL. 2001. A default mode of brain function. Proc Natl Acad Sci USA. 98(2):676–682.
Rugg MD, Curran T. 2007. Event-related potentials and recognition memory. Trends Cogn Sci. 11(6):251–257.
Rushworth MFS, Behrens TEJ, Johansen-Berg H. 2006. Connection patterns distinguish 3 regions of human parietal cortex. Cereb Cortex. 16(10):1418–1430.
Scheperjans F, Eickhoff SB, Hömke L, Mohlberg H, Hermann K, Amunts K, Zilles K. 2008. Probabilistic maps, morphometry, and variability of cytoarchitectonic areas in the human parietal cortex. Cereb Cortex. 18(9):2141–2157.
Scheperjans F, Hermann K, Eickhoff SB, Amunts K, Schleicher A, Zilles K. 2008. Observer-independent cytoarchitectonic mapping of the human superior parietal cortex. Cereb Cortex. 18(4):846–867.
Schott BH, Niklas C, Kaufmann J, Bodammer NC, Machts J, Schütze H. 2011. Fiber density between rhinal cortex and activated ventrolateral prefrontal regions predicts episodic memory performance in humans. Proc Natl Acad Sci USA. 108(13):5408–5413.
Schott BH, Wüstenberg T, Wimber M, Fenker DB, Zierhut KC, Seidenbecher CI, Heinze H-J, Walter H, Duzel E, Richardson-Klavehn A. 2011. The relationship between level of processing and hippocampal-cortical functional connectivity during episodic memory formation in humans. Hum Brain Mapp. 424:407–424.
Schwarze U, Bingel U, Badre D, Sommer T. 2013. Ventral striatal activity correlates with memory confidence for old- and new-responses in a difficult recognition task. PLoS One. 8(3):1–7.
Scimeca J, Badre D. 2012. Striatal contributions to declarative memory retrieval. Neuron. 75(3):380–392.

Sestieri C, Shulman GL, Corbetta M. 2010. Attention to memory and the environment: functional specialization and dynamic competition in human posterior parietal cortex. J Neurosci. 30 (25):8445–8456.
Shimamura AP. 1995. Memory and frontal lobe function. In: Gazzaniga MS, editor. The cognitive neurosciences. Cambridge (MA): MIT Press. p. 803–813.
Shohamy D, Adcock RA. 2010. Dopamine and adaptive memory. Trends Cogn Sci. 14(10):464–472.
Simons JS, Spiers HJ. 2003. Prefrontal and medial temporal lobe interactions in long-term memory. Nat Rev Neurosci. 4(8):637–648.
Stretch V, Wixted JT. 1998. On the difference between strength-based and frequency-based mirror effects in recognition memory. J Exp Psychol Learn Mem Cogn. 24(6):1379–1396.
Stuss DT, Benson DF. 1986. The frontal lobes. New York: Raven.
Suzuki WA, Amaral DG. 1994. Perirhinal and parahippocampal cortices of the macaque monkey: cortical afferents. J Comp Neurol. 350(4):497–533.
Takahashi E, Ohki K, Kim D-S. 2007. Diffusion tensor studies dissociated two fronto-temporal pathways in the human memory system. NeuroImage. 34(2):827–838.
Thiebaut de Schotten M, Dell'Acqua F, Valabregue R, Catani M. 2012. Monkey to human comparative anatomy of the frontal lobe association tracts. Cortex. 48(1):82–96.
Thierry AM, Gioanni Y, Dégénétais E, Glowinski J. 2000. Hippocampo-prefrontal cortex pathway: anatomical and electrophysiological characteristics. Hippocampus. 10(4):411–419.
Thompson-Schill SL, D'Esposito M, Aguirre GK, Farah MJ. 1997. Role of left inferior prefrontal cortex in retrieval of semantic knowledge: a reevaluation. Proc Natl Acad Sci USA. 94(26):14792–7.
Tzourio-Mazoyer N, Landeau B, Papathanassiou D, Crivello F, Etard O, Delcroix N, Mazoyer B, Joilot M. 2002. Automated anatomical labeling of activations in SPM using a macroscopic anatomical parcellation of the MNI MRI single-subject brain. NeuroImage. 15(1):273–289.
Uddin LQ, Supekar K, Amin H, Rykhlevskaia E, Nguyen DA, Greicius MD, Menon V. 2010. Dissociable connectivity within human angular gyrus and intraparietal sulcus: evidence from functional and structural connectivity. Cereb Cortex. 20(11):2636–2646.
Verde M, Rotello C. 2007. Memory strength and the decision process. Mem Cogn. 35(2):254–262.
Vilberg KL, Rugg MD. 2008. Memory retrieval and the parietal cortex: a review of evidence from a dual-process perspective. Neuropsychologia. 46(7):1787–1799.
Vilberg KL, Rugg MD. 2012. The neural correlates of recollection: transient versus sustained fMRI effects. J Neurosci. 32(45): 15679–15687.
Vincent JL, Kahn I, Snyder AZ, Raichle ME, Buckner RL. 2008. Evidence for a frontoparietal control system revealed by intrinsic functional connectivity. J Neurophysiol. 100(6):3328–3342.
Wagner AD, Paré-Blagoev EJ, Clark J, Poldrack RA. 2001. Recovering meaning: left prefrontal cortex guides controlled semantic retrieval. Neuron. 31(2):329–338.
Wagner AD, Shannon BJ, Kahn I, Buckner RL. 2005. Parietal lobe contributions to episodic memory retrieval. Trends Cogn Sci. 9(9): 445–453.
Whitlock DG, Nauta WJH. 1956. Projections, subcortical mulatta, macaca. J Comp Neurol. 106(1):183–212.
Wimber M, Bäuml K-H, Bergström Z, Markopoulos G, Heinze H-J, Richardson-Klavehn A. 2008. Neural markers of inhibition in human memory retrieval. J Neurosci. 28(50):13419–13427.
Yeo BTT, Krienen FM, Sepulcre J, Sabuncu MR, Lashkari D, Hollinshead M, Roffman JL, Smoller JL, Zöllei L, Polimeni JR et al. 2011. The organization of the human cerebral cortex estimated by intrinsic functional connectivity. J Neurophysiol. 106(3): 1125–1165.
Yeterian EH, Pandya DN. 1991. Prefrontostriatal connections in relation to cortical architectonic organization in rhesus monkeys. J Comp Neurol. 312(1):43–67.